Processing and dielectric properties of $ZnTiO_3$ ceramics prepared from nanopowder synthesised by sol-gel technique

Ahcéne Chaouchi[1,*], Malika Saidi[1], Sophie d'Astorg[2,3], Sylvain Marinel[4]

[1]*Laboratoire de Chimie, Appliquée et Génie Chimique de l'Université Mouloud, Mammeri de Tizi-Ouzou, Algérie*

[2]*Laboratoire des Matériaux Céramiques et Procédés Associés, Université de Valenciennes et du Hainaut-Cambrésis, Z.I. du Champ de l'Abbesse, 59600 Maubeuge, France*

[3]*Université de Lille Nord de France, F-59000 Lille, France*

[4]*Laboratoire CRISMAT, UMR 6508 CNRS/ENSICAEN 6 Bd Maréchal Juin, 14050 Caen cedex, France*

Received 26 January 2012; received in revised form 16 April 2012; accepted 29 April 2012

Abstract

$ZnTiO_3$ nanopowders were obtained by sol-gel method. The nanopowders were characterised by means of TGA/DTA analysis, X-ray diffraction, TMA analysis and SEM characterisation. The results show that the crystalline structure of the sol-gel powders was obtained at 600 °C, with crystallite sizes of 10 nm. SEM shows that most of the prepared $ZnTiO_3$ nanopowders are agglomerated. Since agglomeration plays an important role in the sintering of the $ZnTiO_3$ ceramics, different deagglomeration techniques (ultrasonication, pulverisation and attrition milling) were investigated. Dense $ZnTiO_3$ structure was obtained from the attrition milled powder at 1050 °C and its dielectric characteristics were also investigated (ε_r =25, t_ε= -26 ppm/°C and tgδ < 10^{-3} at 1 MHz). The low sintering temperature and the good dielectric properties show promise for the manufacture of multilayered capacitors with internal copper electrodes.

Keywords: *$ZnTiO_3$, sol-gel processes, sintering, dielectric proprieties*

I. Introduction

Passive components such as resonators, filters, oscillators or capacitors play an important role in industrial or commercial electronic systems. The required materials to fabricate these components must exhibit a high dielectric constant, a low dissipation factor (tgδ < 10^{-3}), a small temperature coefficient of the resonant frequency (τ_f) or a small temperature coefficient of the dielectric constant (τ_ε) [1,2], and that at high and hyper frequencies range. Most of the known dielectrics ceramics suitable for those applications require high sintering temperatures (1200–1500 °C) to get well densified materials. This high temperature cycle forbids the use of cheaper base metals, e.g. Cu and Ag, as electrodes, instead of noble metals like Pd and Pt, which are currently employed, and that increases the manufacturing cost, in terms of both money and energy. $ZnTiO_3$ exhibits interesting dielectric properties (ε_r = 20, $Q\times f$ = 30,000 GHz, τ_ε = -55 ppm/°C) [3] that makes it a favourable candidate for high performances passive components. As was established, $ZnTiO_3$ requires high sintering temperature (over 1150 °C) that prevents its usage as a dielectric material for the fabrication of multilayered capacitors with internal copper electrodes, a cheap and common metal. In this work, the main goal is to lower the sintering temperature of $ZnTiO_3$ bellow the copper melting temperature (T_m = 1080 °C). Two basic approaches are commonly used to reduce the sintering temperature:

- addition of glass phase or crystallised materials to act as densification promoter (owing to the formation of a liquid phase which leads to increase the atomic diffusion);
- use of novel powder synthesis method (such as a liquid phase route, e.g. sol-gel) in order to reduce the grain size of the powder and increase its reactivity.

* Corresponding author: tel: +213 26 21 56 51
fax: +213 26 21 29 68, e-mail: *ahchaouchi@yahoo.fr*

The first method (glass phase addition) has been explored in previous studies [4–6] whereas only a few attempts of synthesis $ZnTiO_3$ by liquid route followed by sintering have been reported. In this work, sol-gel method has been developed to produce nanosized $ZnTiO_3$ powder. In addition, $ZnTiO_3$ synthesised by the conventional solid state route has been also produced in order to compare both synthesis methods in terms of sintering temperature, structure, microstructure and dielectrics properties.

II. Experimental

2.1. Sol-gel synthesis (sg-ZT)

The $ZnTiO_3$ gel was synthesised from titanium butoxide, $Ti(OC_4H_9)_4$ (purity of 99.5%) [7]. Titanium butoxide was diluted in absolute ethanol (purity of 99.5%) and stirred for 30 minutes. The obtained solution was then added drop wise to the solution containing ethanol, water and a few drops of HNO_3 and stirred again for 2 hours in order to prepare a homogeneous solution (solution 1). At the same time solution 2 was prepared by total dissolution of zinc acetate, $Zn(OOCCH_3)_2$ (purity of 99.5%) in ethylene glycol. Finally, solution 2 was added drop wise to solution 1, under stirring, during a period of 1 hour, which led to the formation of a homogeneous gel. The obtained gel was dried at 110 °C for 5 hours, ground in a mortar to produce powder and heat treated in air for 2 hours at various temperatures (600 °C, 700 °C, 800 °C, 900 °C and 1000 °C). The whole process is schematically presented in Fig. 1.

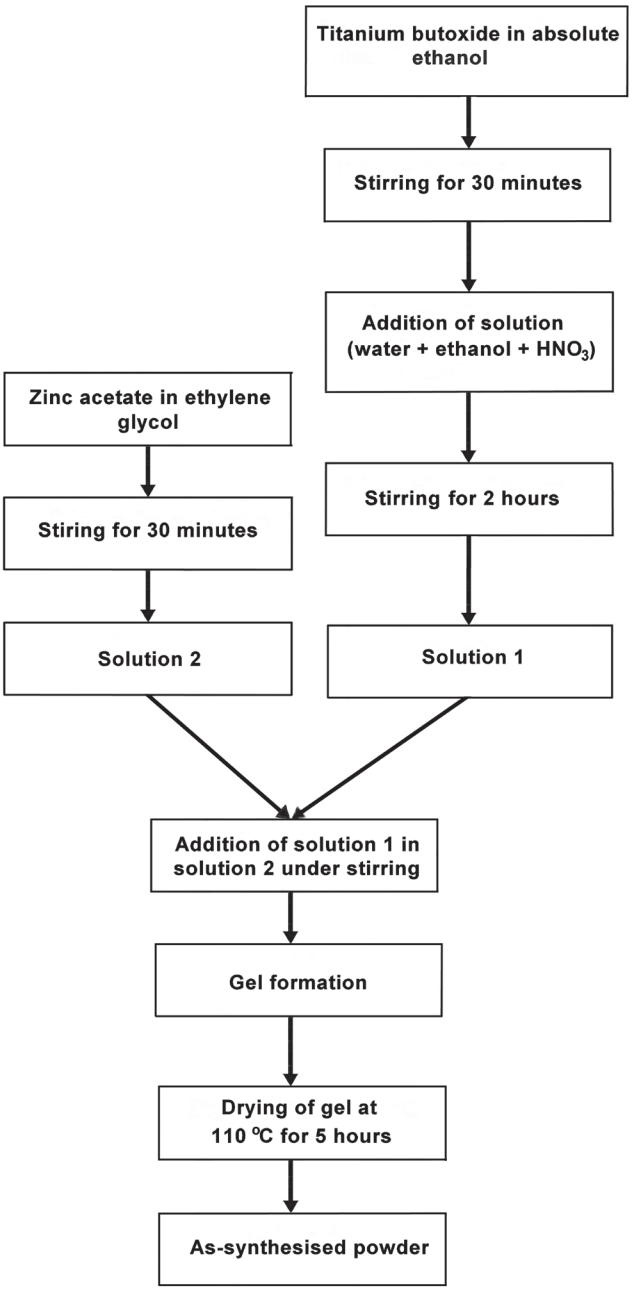

Figure 1. Schematic flow chart of the synthesis of $ZnTiO_3$ powders by sol-gel technique

The molar ratios of the different precursors used were [7]:

$$\frac{[Ti(OC_4H_9)_4]}{[H_2O]} = \frac{1}{1}$$

$$\frac{[Ti(OC_4H_9)_4]}{[C_2H_5OH]} = \frac{1}{25}$$

$$\frac{[Ti(OC_4H_9)_4]}{[Zn(OOCCH_3)_2]} = \frac{1}{1}$$

2.2. Solid state synthesis (ss-ZT)

The precursors, ZnO and TiO_2 (purity >99%), were appropriately weighted according to the Zn/Ti = 1 molar ratio. Mixing was performed in an ammonia solution at pH = 11 using zirconia balls in a teflon jar for 3 hours. These conditions were reported to be optimal for obtaining a stable suspension [8,9]. The slurry was subsequently dried and the obtained powder was manually reground and heat treated in air for 2 hours at various temperatures (700 °C, 800 °C, 900 °C and 1000 °C). The powder was finally reground in an ammoniac solution at pH = 11 for 1 hour, as described previously.

2.3. Processing of $ZnTiO_3$ ceramics

Pressed pellets (8 or 6 mm in diameter and 2 mm thick) were prepared by uniaxial pressing (at a load of about 21 kN) of the synthesised powders mixed with an organic binder (polyvinyl alcohol at 5 vol.%). The green samples were finally sintered in air in a tubular furnace for two hours at a dwell temperature previously determined by thermo-mechanical analysis and heating and cooling rates of 150 °C/h.

2.4. Characterisation of $ZnTiO_3$ samples

The crystalline phase composition was identified by X-ray diffraction (XRD) technique using the CuKα X-ray radiation (Philips X'Pert). Thermo-mechanical analysis was carried out using Setaram TMA 92 instrument and TGA/DTA curves were recorded in air with a Setaram apparatus (TGA92). The densities of the sintered samples were determined using a He pycnometer (Accupyc 1330) and the microstructures were observed using a scanning electron microscope (SEM Philips XL'30).

The dielectric properties were determined using a RLC bridge (PM6306) versus temperature (from -60 °C to 160 °C).

III. Results and discussion

3.1 ZT powder synthesised by sol-gel method

Figure 2 shows TGA/DTA curves of the sol-gel powder and gives the evidence for several phenomena listed bellow.

- An exothermic peak between 277–358 °C is observed on the DTA curve, accompanied by weight loss of 20 wt.% (TGA curve). This can be attributed to the departure of the organic solvents and the combustion of the organic residues.
- An exothermic peak in the temperature range 320–380 °C results from the dehydroxylation of Ti-OH into TiO_2 [10].
- The weight loss ends around 500 °C; no organic matter seems to remain at that temperature.

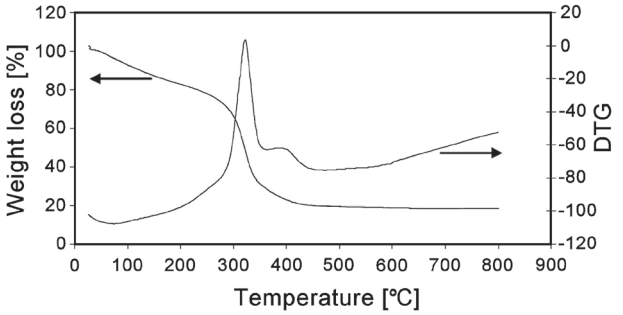

Figure 2. TGA-DTA curves of ZT gel precursor under air

Figure 3a shows the XRD patterns of the sg-ZT powders synthesised by sol-gel method and heat treated at different temperatures. At 600 °C, the powder is composed of the cubic $ZnTiO_3$ phase [JCPDF: 00-039-0190] without any secondary phase. At a higher calcination temperature (700 °C), the cubic $ZnTiO_3$ phase is well crystallised and is the major phase. However, traces of the hexagonal $ZrTiO_3$ phase are already visible in the XRD pattern (see the peak between $2\theta = 30°$ and 36°). At 800 °C, the cubic $ZnTiO_3$ phase disappears and the powder is mainly a mixture of Zn_2TiO_4 and hexagonal $ZnTiO_3$ [PCPDF: 00-014-0033]. At 900 °C, hexagonal $ZnTiO_3$ and Zn_2TiO_4 [PCPDF: 00-018-1487] are still present, but the $ZnTiO_3$/Zn_2TiO_4 ratio is decreased. Finally, at 1000 °C, only Zn_2TiO_4 and TiO_2 (rutile) phases remained. These results are in good agreement with the well known decomposition of the hexagonal $ZnTiO_3$ at 945 °C [11,12].

The average $ZnTiO_3$ crystallite size of the sg-ZT powder was calculated from width of the XRD peaks using the Scherrer equation [13]: $D_{XRD} = 0.9\lambda/\beta\cos\theta$ where D_{XRD} is the average grain size, λ is the X-ray wave-length equal to 0.15406 nm and β is the half-peak width. Figure 4 shows estimated crystallite size as a function of heat treatment. The crystallite size of $ZnTiO_3$ powder is in nanometre range and apparently increases with the temperature. For the $ZnTiO_3$ annealed at 600 °C, the grains size is very fine, about 10 nm, and grew to about 50 nm when the treatment temperature increased to 900 °C.

3.2 ZT powder prepared by solid-state synthesis

The XRD patterns of the ss-ZT powders calcined at different temperatures are shown in the Fig. 3b. At 700 °C, no reaction is taking place since only ZnO and TiO_2 (anatase) precursors are identified. At 800 °C, the XRD pattern is similar to the one observed at 700 °C, when the sol-gel synthesis is used and the cubic $ZnTiO_3$ phase is dominant. At higher calcinations temperatures, the results are as expected - the appearance of the hexagonal $ZnTiO_3$ and Zn_2TiO_4 phases can be detected at

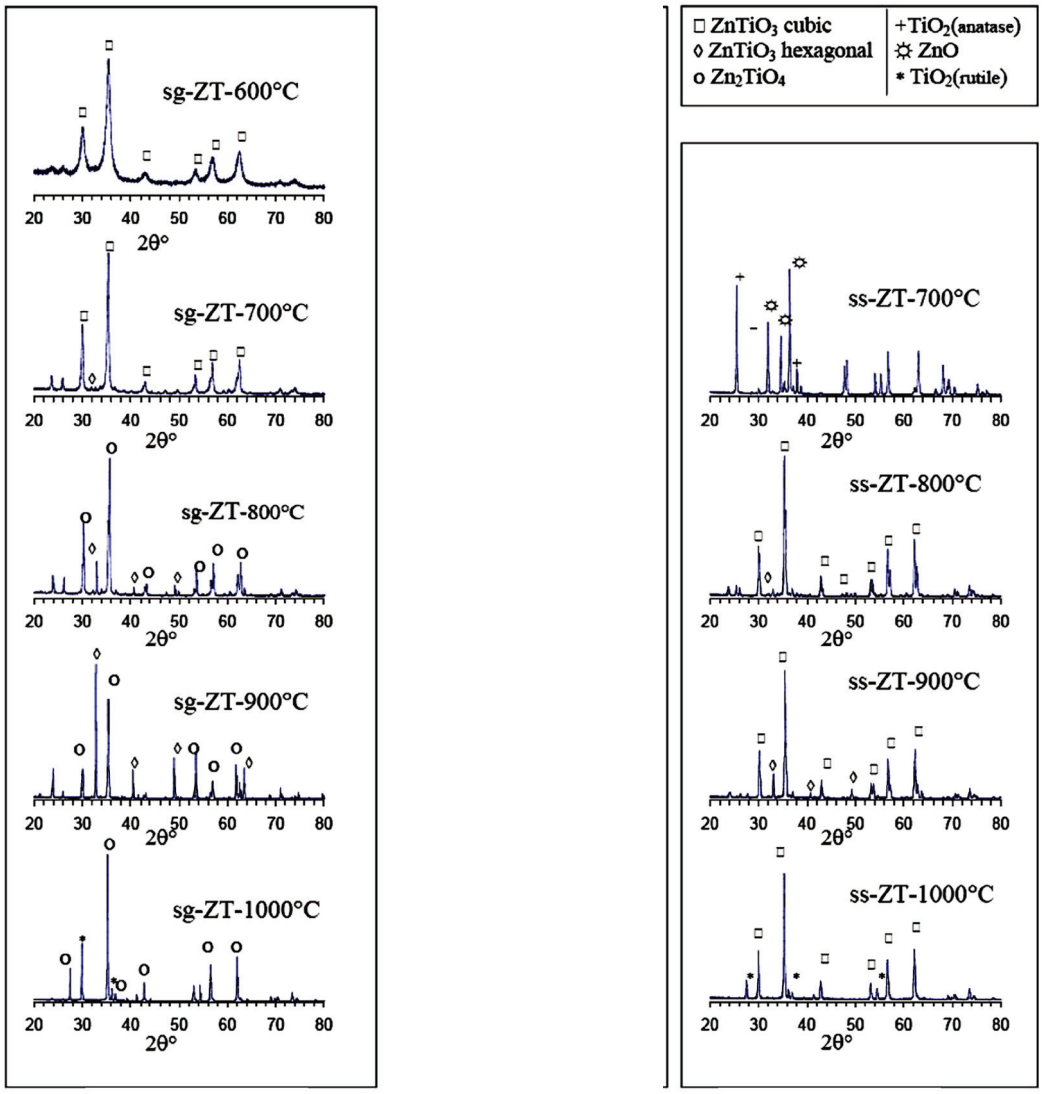

Figure 3. XRD patterns of: a) sg-ZT and b) ss-ZT powders, heat treated at different temperatures

900 °C and the decomposition of the hexagonal $ZnTiO_3$ into TiO_2 (rutile) and Zn_2TiO_4 is occurring at 1000 °C.

3.3 Densification behaviour

The dilatometric curves of the powders are presented in Fig. 5. These experiments were performed for the ss-ZT powder annealed at 800 °C and the sg-ZT powders annealed at different temperatures. The shrinkage of the sg-ZT is not completed at 1150 °C, whereas, the ss-ZT shrinkage ends at 1150 °C. Such phenomenon is attributed to the morphology of the ss-ZT powders. SEM observation shows that the dried sg-ZT gel is agglomerated (Fig. 6a), and the annealed sg-ZT powder consists

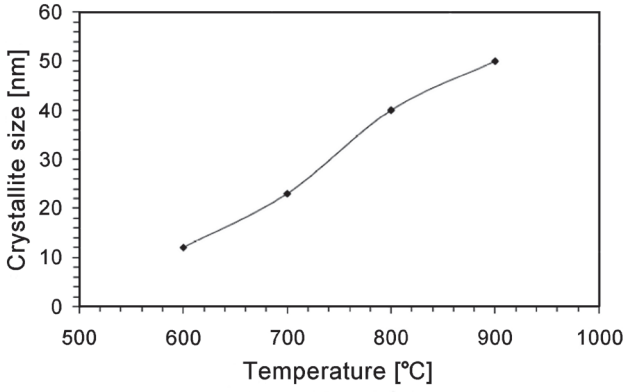

Figure 4. Estimate of the sg-ZT crystallite size as a function of annealing temperature

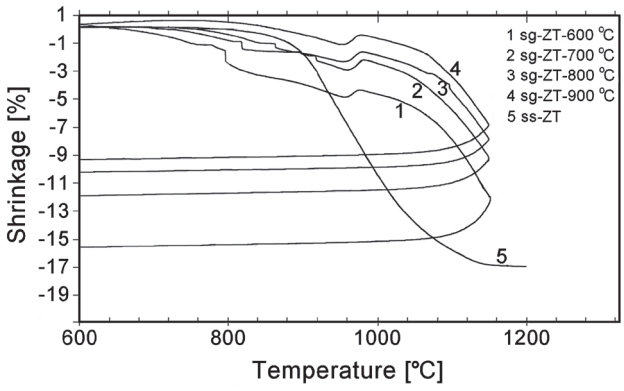

Figure 5. Shrinkage curves versus temperature of sg-ZT heat treated at different temperatures

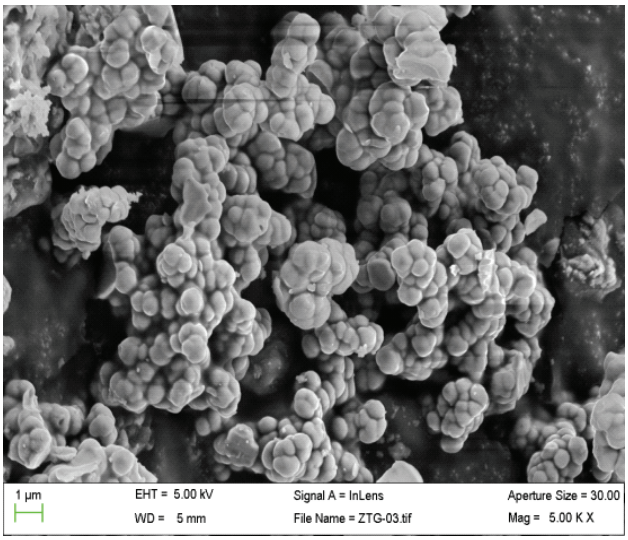

a)

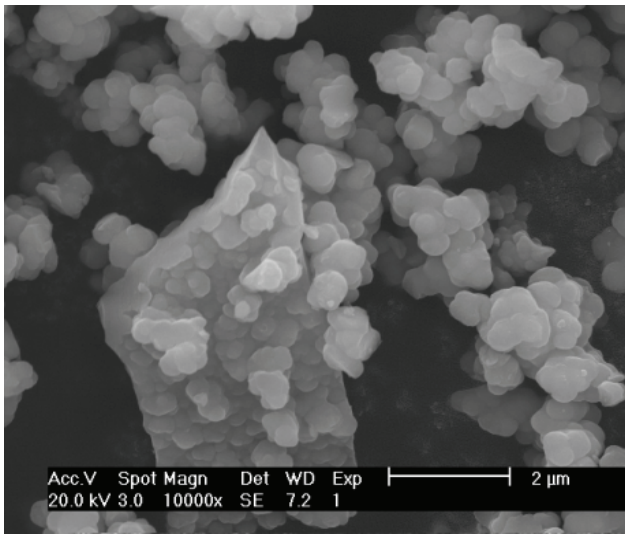

b)

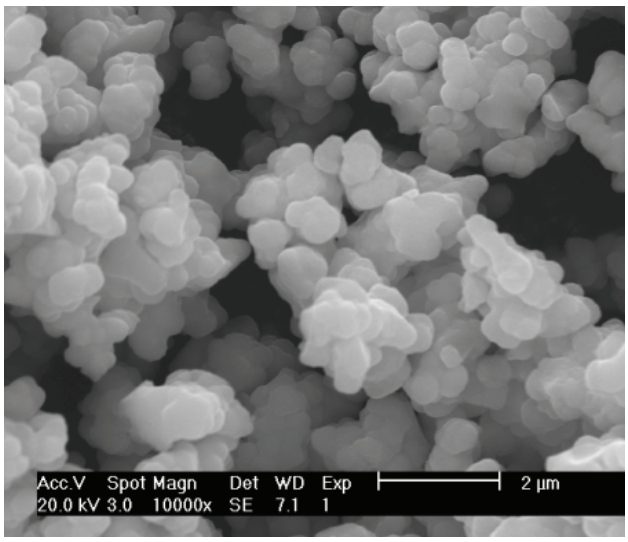

c)

Figure 6. Scanning electron micrographs of sg-ZT powders: a) dried, b) annealed at 600 °C and c) annealed at 700 °C

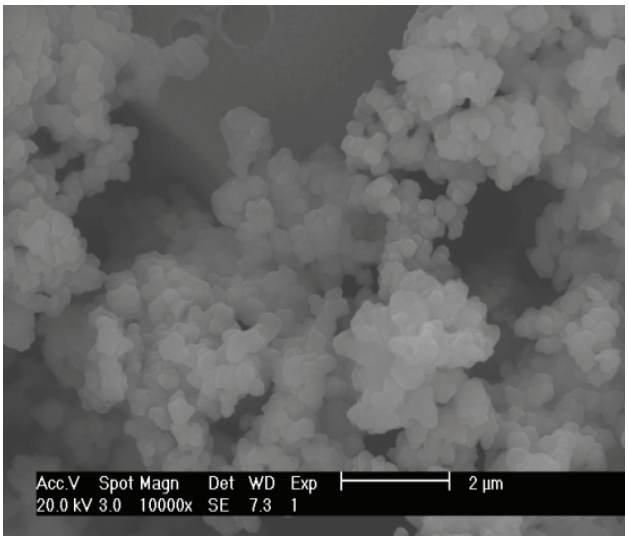

a)

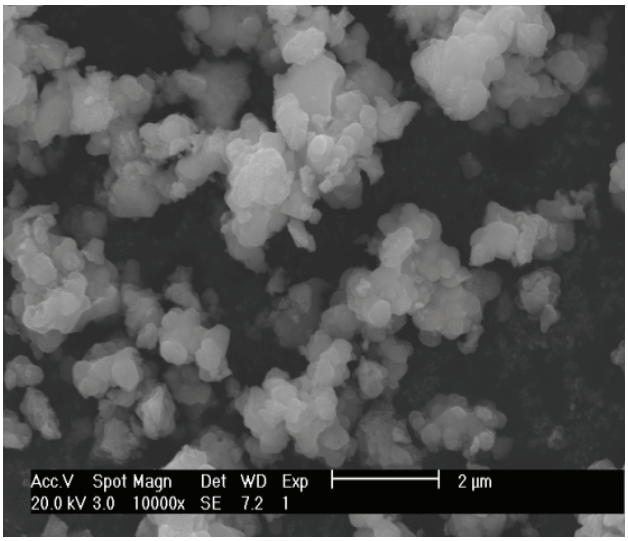

b)

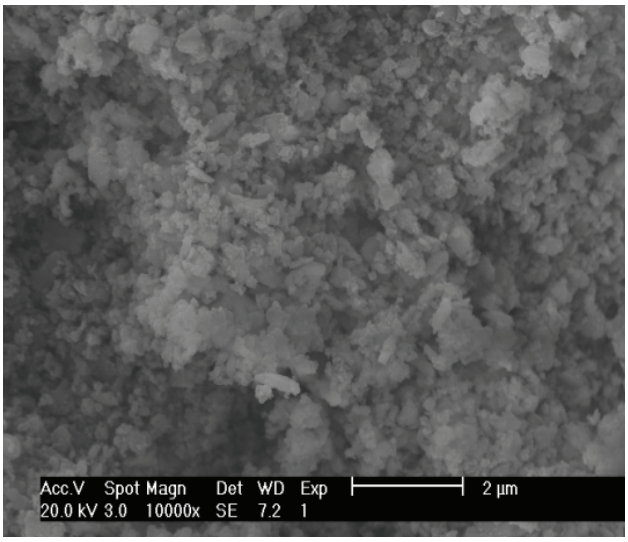

c)

Figure 7. Scanning electron micrographs (SEM) of sg-ZT deagglomerated by various techniques: a) ultrasonication, b) pulverisation and c) attrition milling

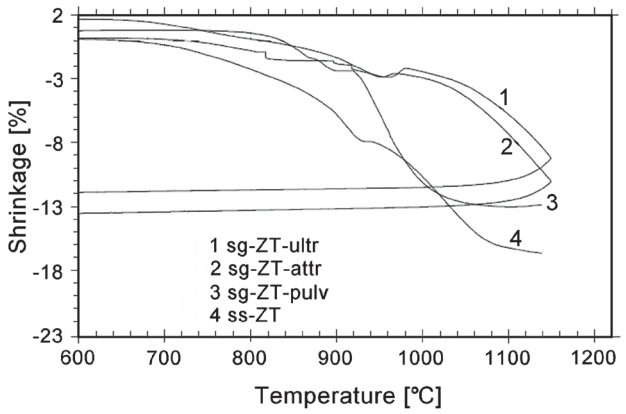

Figure 8. Shrinkage curves versus temperature of sg-ZT grounded by various techniques

of both a fine grain size (200 nm) and large agglomerates (5 μm) (Fig. 6b,c). Even the heat treated sol-gel powders are agglomerated [14,15], the sol-gel method ensures a homogeneous mixing of Zn^{2+} ions and titania sol at a molecular level. It also reduces the diffusion distances between Zn^{2+} ions and TiO_6 octahedra. Therefore, this method combines nano-level compositional homogeneity with high reactivity. The increase of the heat-treatment temperature can greatly increase the agglomeration of the $ZnTiO_3$ nanoparticles. It is well known that the presence of agglomerates plays an important role in the densification process [16] and is the reason for densification difficulties of the sg-ZT samples (Fig. 5.).

The following part is related to the deagglomeration of the sg-ZT powders. It was performed using three different techniques: ultrasonic waves, attrition grinding and pulveriser grinding. Three samples of the powder annealed at 700 °C for 2 hours were prepared. The first one was treated by ultrasound for 30 min and labelled sg-ZT-ultra. The others were ground in an attrition and pulveriser for 1 hour and 45 minutes respectively, and they were named sg-ZT-attr and sg-ZT-pulv, respectively.

Figure 7 shows SEM micrographics of the sg-ZT-ultra, sg-ZT-attr and sg-ZT-pulv powders. The most efficient technique seems to be the attrition. The grains of the sg-ZT-attr are well dispersed and deagglomerated (Fig. 7c). The sg-ZT-pulv powder (Fig. 7a) is partially deagglomerated since agglomerates of 2 μm still remain. Finally, the ultrasonic technique is the least efficient, since no deagglomeration can be observed in the sg-ZT-ultra powder.

As expected, the deagglomeration influences the densification behaviour of the powders. Figure 8 shows the thermo-mechanical analysis of these three powders. The densification behaviour of both sg-ZT-ulttra and sg-ZT-pulv powders remains similar to their behaviour prior to the deagglomeration step because their deagglomeration was not efficient enough. In the case of the sg-ZT-attr powder, the sinterability was improved significantly, since the shrinkage starts at around 850 °C and is completed at 1050 °C. The shrinkage anomaly occurring around 950 °C for the sg-ZT samples (Fig. 4) disappeared completely in the case of the ZTsg-attr sample. This anomaly can be attributed to the morphology of the powder that consists of agglomerates and small grains. The small particles start to sinter at lower temperatures, as can be seen in Figs. 4 and 8, followed by the sintering of larger agglomerates which begins at 950 °C.

The sg-ZT-attr and ss-ZT powders were then sintered at 1050 °C and 1150 °C, respectively. The sg-ZT-attr ceramic (Fig. 9a) presents a heterogeneous microstructure. The average grain size is around 200 nm, while some as large as 1 μm can be observed. The porosity observed on the micrographs confirmed the measured density, which is 92% of theoretical density.

In the case of the ss-ZT, the SEM images show grains between 1 and 5 μm (Fig. 9b) and the obtained density is 97% of theoretical density.

3.4 Dielectric properties

Figure 10 shows the results of the dielectric measurements of both samples versus temperature. The

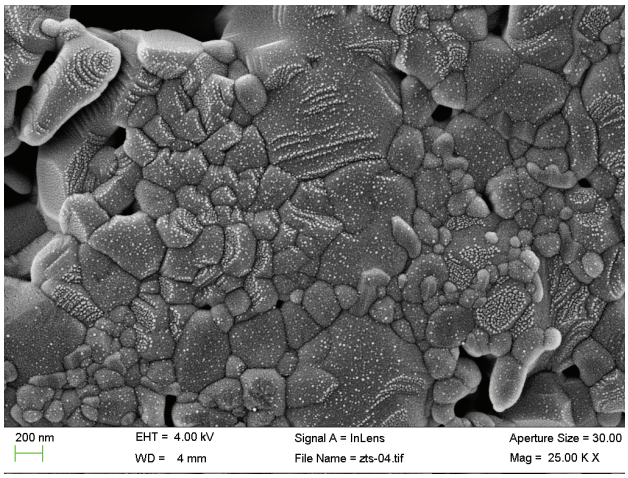

a)

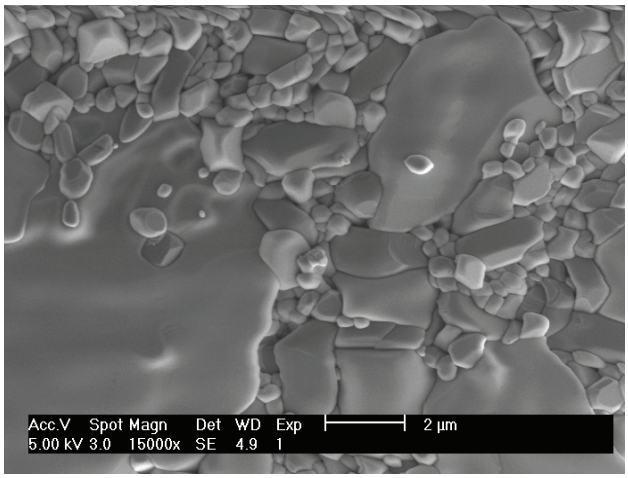

b)

Figure 9. Scanning electron micrographs (SEM) of sg-ZT sintered at 1050 °C and ss-ZT sintered at 1150 °C

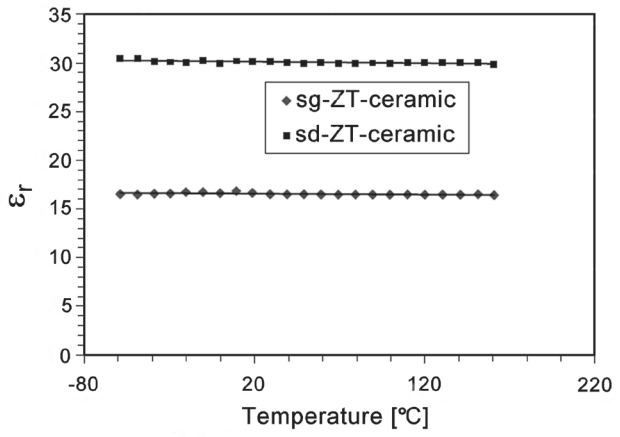

Figure 10. Dielectric characteristics of sg-ZT and ss-ZT ceramics

sg-ZT-attr ceramic exhibits ε_r value of 25 with a low temperature coefficient τ_ε of -26 ppm/°C. This slight deterioration of the dielectric constant is due to the porosity of the sample. The ss-ZT samples exhibits a relative permittivity of 30 and elevated temperature coefficient of the permittivity of -150 ppm/°C.

The dielectric losses and the resistivity of both samples are good: $\mathrm{tg}\delta < 10^{-3}$ and $\rho_i > 10^{13}$ Ω·cm.

IV. Conclusions

In this paper two main advantages of the sol-gel method were highlighted: the low crystallization temperature (600 °C) and the high purity of the sg-ZT powders. The crystalline size of the sg-ZT powders was moreover very small. However, a drawback was the agglomeration of the powder. This phenomenon has a detrimental influence on the densification of the ceramics. Three techniques of deagglomeration were investigated, ultrasonication, pulverisation and attrition milling of which attrition milling was the most efficient. The sg-ZT-attr powder had fewer agglomerates, making the densification of the ceramic easier. Therefore, the sintering temperature could have been lowered to 1050 °C. It means that the deagglomeration procedure allows the sintering temperature to be lowered by 100 °C compared to the sintering temperature needed for the powders produced by the solid state synthesis. Interesting dielectric properties were obtained: $\varepsilon_r = 25$, $\tau_\varepsilon = -26$ ppm/°C and $\mathrm{tg}\delta < 10^{-3}$ at 1 MHz. The low sintering temperature of the sg-ZT-attr makes it sinterable with internal copper electrodes for the production of multilayered capacitors.

References

1. K. Wakino, T. Nischicawa, Y. Ishikawa, H. Tamura, "Dielectric resonator materials and their application for mobile communication systems", *Br. Ceram. Trans. J.*, **89** (1990) 39–43.
2. H. Crremoolanadhan, M.T. Sebashan, P. Mohanan, "High permitivity and low loss ceramics in the $BaOSrO\text{-}Nb_2O_5$ system", *Mater. Res. Bull.*, **30** (1995) 653–658.
3. H.T. Kim, S.H. Kim, X. Nahm, J.D. Dyum, "Microstructure and microwave dielectric properties of modified zinc titanates", *J. Am. Ceram. Soc.*, **82** (1999) 3043–3048.
4. S.F. Wang, F. Gu, M.K. Lu, C.F. Song, S.W. Liu, D. Xu, D.R. Yuan, "Preparation and characterization of sol-gel derived $ZnTiO_3$ nanocrystals", *Mater. Res. Bull.*, **38** (2003) 1283–1288.
5. A. Chaouchi, M. Aliouat, S. Marinel, S. d'Astorg, H. Bourahla, "Effects of additives on the sintering temperature and dielectric properties of $ZnTiO_3$ based ceramic", *Ceram. Int.*, **33** (2007) 245–248.
6. A. Chaouchi, S. d'Astorg, S. Marinel, M. Aliouat, "$ZnTiO_3$ ceramic sintered at low temperature with glass phase addition for LTCC applications", *Mater. Chem. Phys.*, **103** (2007) 106–111.
7. A. Chaouchi, S. Marinel, M. Aliouat, S. d'Astorg, "Low temperature sintering of $ZnTiO_3/TiO_2$ based dielectric with controlled temperature coefficient", *J. Eur. Ceram. Soc.*, **27** (2007) 2561–2566.
8. S. Liufu, H. Xiao, Y. Li, "Investigation of of PEG adsorption on the surface of zinc oxide nanoparticles", *Powder Technol.*, **145** (2004) 20–24.
9. Y.K. Leog, B. Cong, "Critical zeta potential and the Hamaker constant of oxides in water", *Powder Technol.*, **134** (2003) 249–254.
10. E. Hosono, S. Fujihara, M. Onuki, T. Kimura, "Low-temperature synthesis of nanocrystalline zinc titanate materials with high specific surface area", *J. Am. Ceram. Soc.*, **87** [9] (2004) 1785–1788.
11. Y.-S. Chang, Y.-H. Chang, I.-G. Chen, Y.-L. Chai, S.-Wu, T.-H. Fang, "Synthesis, formation and characterization of $ZnTiO_3$ ceramics", *Ceram. Int.*, **30** (2004) 2183–2189.
12. J. Yang, J.H. Swisher, "The phase stability of $Zn_2Ti_3O_8$", *Mater. Charact.*, **37** (1996) 153–159.
13. E.R. Leite, J.A. Valera, E. Longo, C.A. Paskocimas, "Influence of polymerization on the synthesis of $SrTiO_3$: Part II. Particle and agglomerate morphologies", *Ceram. Int.*, **21** (1995) 153–158.
14. I.M.G. Dos Santos, E. Longo, J.A. Varela, E.R. Leite, "Sintering of tin oxide processed by slip casting", *J. Eur. Ceram. Soc.*, **20** (2000) 2407–2413.
15. W.F.M. Groot Zeverg, A.J.A. Winnubst, G.S.A.M. Theunissen, A.J. Burggraaf, "Powder preparation and compaction behaviour of fine-grained Y-TZP", *J. Mater. Sci.*, **25** (1990) 3449–3455.
16. B.D. Cullity, *Element of X-ray Diffraction*, second ed., Addison Wesley, Publishing Company Inc, MA, 1978.